

# Multiport E-band Wavelength Equalizer

Nicolas K. Fontaine<sup>(1)</sup>, Ian D. Phillips<sup>(2)</sup>, Wladek Forysiak<sup>(2)</sup>, Lauren Dallachiesa<sup>(1)</sup>, Mikael Mazur<sup>(1)</sup>, Roland Ryf<sup>(1)</sup>, Haoshuo Chen<sup>(1)</sup>, and David T. Neilson<sup>(1)</sup>

<sup>(1)</sup> Nokia Bell Labs, Murray Hill, NJ, 07974 USA, [nicolas.fontaine@nokia-bell-labs.com](mailto:nicolas.fontaine@nokia-bell-labs.com)

<sup>(2)</sup> AIPT, Aston University, Birmingham, B4 7ET, UK, [i.phillips@aston.ac.uk](mailto:i.phillips@aston.ac.uk)

**Abstract** We demonstrate a 4-port E-Band (1380nm-1470nm) wavelength equalizer with insertion loss of 4 to 6dB. We use polarization diverse piston phase on the LCoS for attenuation which can enable high port count equalizers. ©2023 The Author(s)

## Introduction

Network capacity growth has been driven by the increasing use of online and Cloud based applications. These substantial growth rates have previously been accommodated by increasing the spectral efficiency of systems using C-Band optical amplifiers, with system capacity growing from a few hundred Gb/s to tens of Tb/s over the last two decades<sup>[1]</sup>. However as widely deployed high data-rate C-band optical transmission systems reach their Shannon capacity limit, a number of possible solutions are being investigated<sup>[1]-[4]</sup>. This includes (1) increasing the optical constellation order and/or baud-rate, (2) increasing the number of spatial channels, (3) increasing the optical bandwidth. Focusing our attention to option (3), a number of key components are required to make this a reality, including low noise optical amplifiers<sup>[5]-[7]</sup>, wavelength selective switches and dynamic optical filters or wavelength equalizers. Previously a 36-THz wavelength selective switch (WSS) was demonstrated covering the O-L bands<sup>[8]</sup>. Systems with large numbers of parallel spatial channels, option (2) above, will require large numbers of parallel wavelength equalizers<sup>[1]</sup>.

In this work, we focus on demonstrating a multiport (up to 90) wide-band (90nm) optical wavelength equalizer operating in the E-band which would be needed for E-band systems, in particular SDM systems with many spatial channels. This equalizer uses a piston phase attenuation mechanism which could allow very large numbers of parallel ports.

## Wavelength Equalizer Design

The wavelength equalizer is designed to provide dynamic optical filtering and flexible gain equalisation across the E-band (1380nm to 1470nm), while simultaneously supporting multiple ports. The wavelength equalizer optical system consists

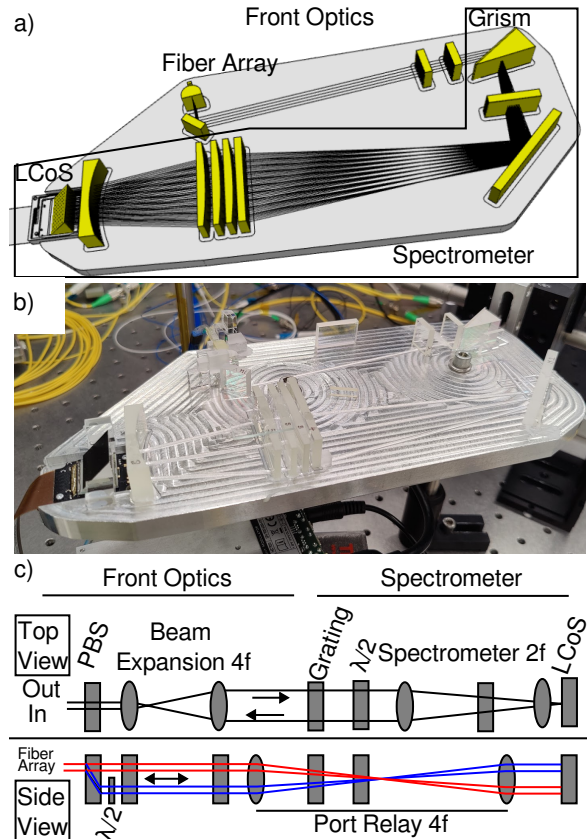


**Fig. 1:** a) Ray simulation and mechanical model of the wavelength equalizer. System utilizes cylindrical optics. Dispersion grating is mounted on prism to linearize spectrum. b) Image of packaged blocker assembled on base plate. c) Schematic for wavelengths (top view) and ports (side view).

of vertical and horizontal anamorphic optical systems, and is similar to previous designs used for other bands<sup>[9]</sup>. It can also be divided into a front optics section and a spectrometer section. The front optics is responsible for implementing the polarization diversity and expanding the beams onto the grating. The spectrometer section consists of a 1200l/mm grating bonded to a 30-degree low index prism to provide some linearisation of the dispersed spectrum, followed by a multi-element lens to image the spectrum on the LCoS. The lens system utilizes a single high in-

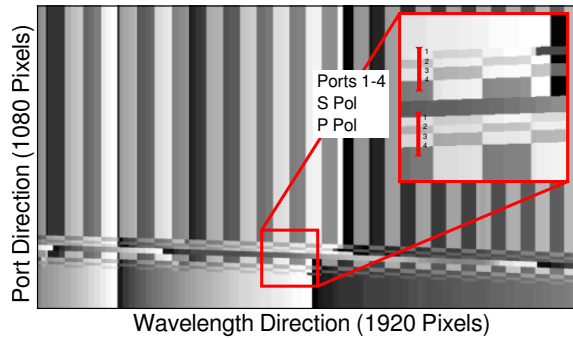


**Fig. 2:** Typical hologram displayed on the LCoS. Attenuation is introduced by pistoning the phase. Each port covers 8 vertical pixels and most of LCoS is unused. Due to availability limitations of the polarization optics we could only calibrate and measure 4 ports.

dex low dispersion glass. Chromatic aberrations in the system are relatively small and can be compensated in the spectrometer section by introducing small tilts and offsets into the optical system.

### Operation and Results

A vertical cylindrical lens based relay that traverses both the front optics and spectrometer relays the ports to the LCoS. The optical system design with its corresponding mounting plate is shown in Figure 1. The grating used was 1200 lines per mm optimised for O-band transmission, but by shifting the incidence angle demonstrates efficiency above 90% and fabricated on fused silica ( $n=1.44$ ), representing 1dB double pass loss. A custom grating designed for E-Band operation could likely reduce insertion loss of the system by an additional 0.5dB.

A prism ( $n=1.49$ ) is bonded with UV epoxy to the grating output allowing the spectrum to be linearised allowing uniform performance over the wavelength range. The angle was chosen such that none of the wavelengths emerged at normal incidence, thus preventing back reflections from the prism and also allowing dispersion variation at the LCoS to be minimised. The input port array consists of a  $2 \times 16$  port fibre array on 127- $\mu\text{m}$  pitch cylindrical micro lenses. Each of the 16 fiber arrays corresponds to an input or output port. Polarisation diversity is implemented by using extra spatial locations on the LCoS. After the fiber array, a  $\text{YVO}_4$  walk-off vertically offsets the 4 ports by 1-mm. One polarization is rotated by 90 degrees with a half waveplate such that all beams are vertically polarized. After the grating, another half-wave plate rotates the beams to 45 degree polarization.

On the LCoS, each of the polarizations are vertically offset spatially such that each polarization

can be controlled individually to adjust the polarization dependent loss. LCoS devices only modulate the phase of one polarization. Attenuation function is obtained via polarization rotation introduced by pistoning the phase on the LCoS followed by polarization filtering in the polarization optics. A C-band blocker array used a similar attenuation technique<sup>[10]</sup>. The wavelength equalizer optical system and LCoS array supports up to 90 ports<sup>[9]</sup>, but due to availability limitations of the polarization optics (4 ports) and the fiber array (16 ports), we could only calibrate and use 4-ports. Figure 2 shows the port locations on the LCoS which are duplicated vertically for the two polarizations. Typical WSSs use blazed gratings to attenuate, however, when the vertical extent of the beams are only 30  $\mu\text{m}$  or 5 vertical pixels per port, the beam steering gratings introduce phase wraps that cause spectral ripple. Pistoning phase is the only way to achieve a huge number of ports, potentially up to the number of pixels on the LCoS.

### Calibration, alignment and measurement

To characterize and calibrate the wavelength equalizer we used a swept wavelength interferometer supporting multiple ports, which can simultaneously measure the Jones elements on all the ports in about 1.3 seconds. It is adapted from ref<sup>[11]</sup> and similar to the swept wavelength systems used to characterize the 36-THz bandwidth WSS in ref<sup>[8]</sup>.

Calibration can be accomplished simultaneously for all ports and comprises: 1) vertical port location identification, 2) wavelength registration, and 3) attenuation calibration. Vertical ports are found by scanning a 4 pixel stripe vertically through the entire vertical direction. Vertical ports are identified when the reflected power changes. Wavelength registration is accomplished by placing a horizontal square pattern on the LCoS and marking the pixel number for each spectral transition. For attenuation calibration, the procedure pistons the phase across the entire channel to generate a lookup table. Since there are two polarization spatially separated on the LCoS, there is an independent calibration for each polarization.

Figure 3 shows the measurement of the four channels with full power and with full attenuation. The attenuation available for phase pistoning induced polarization rotation is a function of the quality of the polarization optics. We used polar-

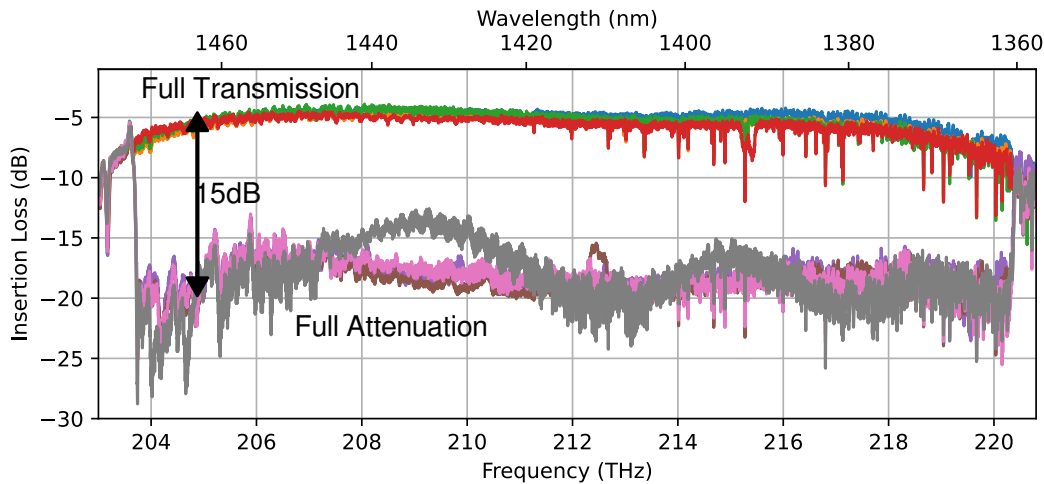


Fig. 3: Full transmission bandwidth showing the range of attenuation for the different ports.

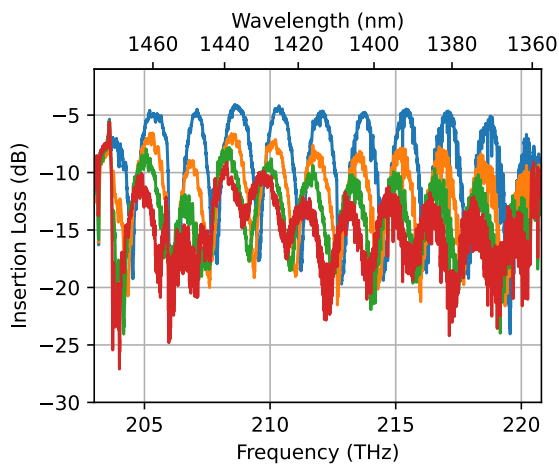


Fig. 4: Example of independent filtering across the E-band. Each colour corresponds to a different port.

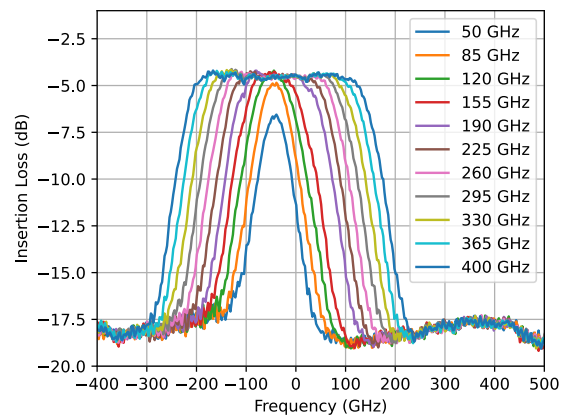


Fig. 5: Filter shapes for various passband widths from 50GHz to 400GHz.

ization optics optimized for 1550 nm, which reduced the maximum attenuation somewhere between 15-20-dB. Using optimized polarization optics in the E-band could improve the maximum attenuation. The as tested device was an unsealed free-space design, and water absorption contributes to the insertion loss. The dips and excess attenuation above 214 THz are from water absorption. In a sealed device, these dips should vanish and insertion loss would be lower.

Figure 4 shows different arbitrary attenuation patterns applied to different ports to show that the channels are independent. The crosstalk between channels is 40-dB. Passband bandwidths for different programmed channel bandwidths from 50GHz to 400GHz are shown in Figure 5. The equalizer can produce a 100GHz full width 3-dB filter shape which is sufficient for gain equalization in optical transmission systems.

### Discussion and Conclusions

We have demonstrated a multi-port wavelength equalizer for the E-band. It utilizes a piston

phase shift between polarization diverse beams on the LCoS to create polarization rotation which is translated into attenuation. This scheme uses fewer pixels than more conventional attenuation holograms, which potentially allows scaling to a large number of ports. This system addresses issues for the exploitation of new wavelength bands and a very large number of parallel spatial channels, which are both critical for future optical capacity scaling<sup>[1]</sup>.

### Acknowledgements

IDP and WF are supported by UK EPSRC grant EP/V000969/1.

### References

- [1] P. J. Winzer, D. T. Neilson, and A. R. Chraplyvy, "Fiber-optic transmission and networking: The previous 20 and the next 20 years (invited)", *Opt. Express*, vol. 26, no. 18, pp. 24 190–24 239, Sep. 2018. DOI: 10.1364/OE.26.024190.
- [2] A. Ferrari, A. Napoli, J. Fischer, *et al.*, "Assessment on the achievable throughput of multi-band ITU-T G.652.D fiber transmission systems", *J. Lightw. Technol.*, vol. 38,

- no. 16, pp. 4279–4291, Aug. 2020. DOI: 10.1109/JLT.2020.2989620.
- [3] T. Hoshida, V. Curri, L. Galdino, *et al.*, “Ultrawideband systems and networks: Beyond C+L-band”, *Proceedings of the IEEE*, vol. 110, no. 11, pp. 1725–1741, 2022. DOI: 10.1109/JPRDC.2022.3202103.
- [4] J. Renaudier, A. Napoli, M. Ionescu, *et al.*, “Devices and fibers for ultrawideband optical communications”, *Proceedings of the IEEE*, vol. 10, no. 11, pp. 1742–1759, 2022. DOI: 10.1109/JPRDC.2022.3203215.
- [5] P. Hazarika, M. Tan, A. Donodin, *et al.*, “E-, S-, C- and L-band coherent transmission with a multistage discrete Raman amplifier”, *Optics Express*, vol. 30, no. 24, pp. 43 118–43 126, 2022. DOI: 10.1364/OE.474327.
- [6] A. Donodin, V. Dvoyrin, E. Manuylovich, *et al.*, “Bismuth doped fibre amplifier operating in E- and S- optical bands”, *Optical Materials Express*, vol. 11, no. 1, pp. 127–135, 2021. DOI: 10.1364/OME.411466.
- [7] J. W. Dawson, L. S. Kiani, P. H. Pax, *et al.*, “E-band Nd<sup>3+</sup> amplifier based on wavelength selection in an all-solid micro-structured fiber”, *Optics express*, vol. 25, no. 6, pp. 6524–6538, 2017. DOI: 10.1364/OE.25.006524.
- [8] N. K. Fontaine, M. Mazur, R. Ryf, H. Chen, L. Dalchiesa, and D. T. Neilson, “36-THz bandwidth wavelength selective switch”, in *2021 European Conference on Optical Communication (ECOC)*, IEEE, 2021, pp. 1–4. DOI: 10.1109/ECOC52684.2021.9606114.
- [9] M. Mounaix, N. K. Fontaine, D. T. Neilson, *et al.*, “Arbitrary vector spatiotemporal beamshaping: any amplitude, phase and polarization at any delay”, in *Complex Light and Optical Forces XVII*, D. L. Andrews, E. J. Galvez, and H. Rubinsztein-Dunlop, Eds., International Society for Optics and Photonics, vol. PC12436, SPIE, 2023, PC1243603. DOI: 10.1117/12.2652118.
- [10] Y. Sakurai, M. Kawasugi, Y. Hotta, *et al.*, “LCOS-based wavelength blocker array with channel-by-channel variable center wavelength and bandwidth”, *IEEE Photonics Technology Letters*, vol. 23, no. 14, pp. 989–991, 2011. DOI: 10.1109/LPT.2011.2148702.
- [11] G. VanWiggeren and D. Baney, “Swept-wavelength interferometric analysis of multiport components”, *IEEE Photonics Technology Letters*, vol. 15, no. 9, pp. 1267–1269, Sep. 2003. DOI: 10.1109/1pt.2003.816663.